



Immobilization of D-allulose 3-epimerase into magnetic metal–organic framework nanoparticles for efficient biocatalysis

Kai Xue^{1,2} · Chun-Li Liu^{1,2} · Yankun Yang^{1,2} · Xiuxia Liu^{1,2} · Jinling Zhan^{1,2} · Zhonghu Bai^{1,2}

Received: 6 December 2021 / Accepted: 6 June 2022 / Published online: 24 June 2022
© The Author(s), under exclusive licence to Springer Nature B.V. 2022

Abstract

D-allulose is a rare low-calorie sugar that has many fundamental biological functions. D-allulose 3-epimerase from *Agrobacterium tumefaciens* (AT-DAEase) catalyzes the conversion of D-fructose to D-allulose. The enzyme has attracted considerable attention because of its mild catalytic properties. However, the bioconversion efficiency and reusability of AT-DAEase limit its industrial application. Magnetic metal–organic frameworks (MOFs) have uniform pore sizes and large surface areas and can facilitate mass transport and enhance the capacity for enzyme immobilization. Here, we successfully encapsulated cobalt-type AT-DAEase into the cobalt-based magnetic MOF ZIF-67@Fe₃O₄ using a self-assembly strategy. We confirmed the immobilization of enzyme AT-DAEase and characterized the enzymatic properties of the MOF-immobilized AT-DAEase@ZIF-67@Fe₃O₄. The AT-DAEase@ZIF-67@Fe₃O₄ nanoparticles had higher catalytic activity (65.1 U mg⁻¹) and bioconversion ratio (38.1%) than the free AT-DAEase. The optimal conditions for maximum enzyme activity of the AT-DAEase@ZIF-67@Fe₃O₄ nanoparticles were 55 °C and pH 8.0, which were significantly higher than those of the free AT-DAEase (50 °C and pH 7.5). The AT-DAEase@ZIF-67@Fe₃O₄ nanoparticles displayed significantly improved thermal stability and excellent recycling performance, with 80% retention of enzyme activity at a temperature range of 45–70 °C and > 45% of its initial activity after eight cycles of enzyme use. The AT-DAEase@ZIF-67@Fe₃O₄ nanoparticles have great potential for large-scale industrial preparation of D-allulose by immobilizing cobalt-type AT-DAEase into magnetic MOF ZIF-67@Fe₃O₄.

Keywords D-allulose · D-fructose · D-allulose 3-epimerase · Immobilization · Magnetic metal–organic frameworks

✉ Chun-Li Liu
liuchunli201774@126.com

✉ Zhonghu Bai
baizhonghu@jiangnan.edu.cn

Kai Xue
429029579@qq.com

Yankun Yang
yangyankun@jiangnan.edu.cn

Xiuxia Liu
liuxiuxia@jiangnan.edu.cn

Jinling Zhan
zjinling@jiangnan.edu.cn

¹ National Engineering Research Center of Cereal Fermentation and Food Biomanufacturing, Jiangnan University, Lihu Road No. 1800, Binhu District, Wuxi 214122, Jiangsu, People's Republic of China

² Jiangsu Provincial Research Center for Bioactive Product Processing Technology, Jiangnan University, Lihu Road No. 1800, Binhu District, Wuxi 214122, Jiangsu, People's Republic of China

Introduction

D-allulose is a C-3 epimer of D-fructose. This rare sugar has attracted much attention because of its many fundamental biological functions (Tseng et al. 2014). It has approximately 70% of the sweetness of sucrose but produces few calories because it inhibits hepatic lipogenic enzymes (Matsuo et al. 2002). Foods containing D-allulose show higher antioxidant activities than those without D-allulose (Sun et al. 2008). D-allulose has been 'generally recognized as safe' by the Food and Drug Administration (Zhang et al. 2013). Owing to these advantages over other sugars, D-allulose has been widely applied in food additives, medicine, cosmetics, flavors, and other preparations (Tseng et al. 2014). D-allulose has become an ideal substitute for sucrose, especially for obese patients or people seeking diet-related weight loss. However, D-allulose is rarely encountered in nature, and its chemical synthesis is cumbersome, costly, and time-consuming (Patel et al. 2018). With the sustainable development of green chemistry and biotechnologies, enzymatic catalysis

may prove valuable for the production of D-allulose because biocatalysts naturally evolve and have high selectivity (Sheldon and Woodley 2018).

Biological processes, such as enzymatic catalysis using ketose epimerase and aldose isomerase or other microbial reactions, are feasible for the synthesis of D-allulose (Kim et al. 2006b, a; Zdarta et al. 2018). In recent years, the bio-production of D-allulose from the naturally available sugar D-fructose using D-allulose 3-epimerase (DAEase) has proven to be a potential method (Itoh et al. 1994; Zhang et al. 2013). DAEase for C-3 epimerization of D-fructose to D-allulose was identified and characterized from *Agrobacterium tumefaciens* (*A. tumefaciens*) (Kim et al. 2006b, a), *Clostridium cellulolyticum* (*C. cellulolyticum*) H10 (Mu et al. 2011), *Ruminococcus* sp. (Zhu et al. 2012), and *Bacillus* sp. (Patel et al. 2021), and metagenomics (Patel et al. 2020). DAEase from *A. tumefaciens* (AT-DAEase) is more thermally stable than other DAEases and is potentially applicable for the biosynthesis of D-allulose (Tseng et al. 2014). Although AT-DAEase has been successfully applied to produce D-allulose, its high costs and low bioconversion efficiency limit its use in industrial applications (Pei et al. 2013). Immobilizing enzymes to biosynthesize products can improve their bioconversion efficiencies and reduce production process costs for the recyclability of the enzymes (Dicosimo et al. 2013). Various methods of immobilizing enzymes have been described, such as cross-linking and entrapment into particles and binding to a solid support (Franssen et al. 2013). DAEase immobilized using artificial oil bodies exhibited higher effective catalytic activity and reusability (Tseng et al. 2014). DAEases were also immobilized on graphene oxide (Dedania et al. 2017), Duolite A568 beads (Lim et al. 2009), Fe₃O₄ (Patel et al. 2018), and Co₃(PO₄)₂ nanosheets (Zheng et al. 2018). These immobilizations improved the physical and catalytic properties. However, the activity of DAEase decreased when the cross-linker glutaraldehyde was used. The development of new materials and methods for immobilizing DAEase is urgently needed to achieve high catalytic efficiency, stability, and reusability.

Metal–organic frameworks (MOFs) have attracted tremendous interest in enzyme immobilization research owing to their ultra-high porosity, large hierarchical surface area, and excellent thermal/chemical stability (Li et al. 2016; Meshkat et al. 2020; Yogapriya and Datta 2020). Some enzymes working need harsh conditions which normally cause loss of the catalytic activity, fortunately, MOFs could enable the retention of the enzyme activity (Liang et al. 2015; Mao et al. 2020; Meshkat et al. 2020). Over the past few years, various enzymes have been successfully prepared to reduce the catalytic activity caused by harsh conditions via various methods using different MOF matrices as supports (Lian et al. 2017; Wu et al. 2015). Generally, there are four strategies for enzyme immobilization with MOFs:

surface adsorption onto MOFs, covalent/coordination bonding with MOFs, coordination bonding, and de novo encapsulation (Wu et al. 2015). Among these, encapsulation of enzymes is the preferred method for synthesizing enzyme-MOF.

Zeolitic imidazolate frameworks (ZIFs) are a subfamily of MOFs with a zeolite topology in which the metal clusters are connected by imidazole linkers. In particular, ZIF-67 has become a perfect support material because of its unique properties of different pore sizes, high surface area, cobalt transition metal, and rich N resources (Kaneti et al. 2017). Co-dependent nitrile hydratase (NHase) was successfully encapsulated in ZIF-67, and the synthesized NHase@ZIF-67 nanoparticles displayed significantly improved thermal stability (Pei et al. 2020). DAEase is also a co-dependent enzyme. The cobalt (II) ion (Co) is crucial for catalysis as an anchor for the substrate and can maximize the activity of DAEase through its isomerism effect (Kim et al. 2006b, a). However, to our knowledge, the use of ZIF-67 to immobilize DAEase has not yet been reported. Furthermore, magnetic nanoparticles could enable easy separation of the biocatalyst enzyme from the reaction system using a magnet, facilitating the reusability of the catalyst (Talekar et al. 2012; Zdarta et al. 2018). Therefore, using the magnetic MOF ZIF-67 containing cobalt (II) ion as the scaffold to spatially colocalize and positional assemble DAEase is an efficient way to immobilize DAEase for D-allulose production.

In this study, we overexpressed the AT-DAEase enzyme in *Escherichia coli* (*E. coli*) BL21 (DE3) and immobilized the enzyme by encapsulating it into the magnetic metal–organic framework ZIF-67@Fe₃O₄ for D-allulose production. First, we overexpressed and purified the enzyme AT-DAEase from the reconstituted strain and simultaneously prepared the MOF material ZIF-67@Fe₃O₄. Then, we characterized the magnetic Fe₃O₄, MOF material ZIF-67@Fe₃O₄, and immobilized AT-DAEase@ZIF-67@Fe₃O₄. Finally, we evaluated the bioconversion efficiency, stability, and reusability of the immobilized AT-DAEase@ZIF-67@Fe₃O₄ by comparing it with the free enzyme AT-DAEase.

Materials and methods

Construction of AT-DAEase expression plasmid

The DAE gene (GenBank ID: WP_010974125.1) fragment encoding AT-DAEase from *A. tumefaciens* was chemically synthesized after codon optimization by Suzhou Genewit Biological Technology Co. Ltd. (Suzhou, China). The amplified product of 870 bp was obtained using the template of the synthesized gene and the primers (FP: 5-CGCGGATCCATG AAGCACGGCATCTACTATAG and RP: AACTGCAGTTA ACCGCCAGCACAAAGCGG), and then cloned into a

6×His-tagged pRSFDuet-1 vector to obtain the recombinant plasmid pRSF-DAE. A single isolated colony was picked and sent to Suzhou Genewiz Biological Technology Co. Ltd. for sequence verification.

Expression and purification of recombinant protein

After sequencing, the plasmid pRSF-DAE was transformed into *E. coli* BL21 (DE3) for protein production. Single isolated colonies were inoculated into 5 mL Terrific Broth (TB) medium (Sangon Biotech Co., Ltd., Shanghai, China) with the addition of 50 µg/mL kanamycin and shaken in a 220 rpm incubator at 37 °C overnight. The culture was transferred into 200 mL TB medium, induced by 0.5 mM isopropyl- β -D-thiogalactopyranoside (IPTG; Sangon Biotech Co., Ltd.) and further incubated at 18 °C for protein expression.

After 18 h of induction, the cells were harvested by centrifugation at 8000 g for 10 min at 4 °C. They were resuspended in 50 mM PBS lysis buffer (pH 7.5) and crushed with a high-pressure cell crusher (Union-Biotech Co., Ltd., Shanghai, China). The lysate was centrifuged at 10,000 g for 10 min at 4 °C to obtain the supernatant. The protein was purified by loading the supernatant on a Ni-NTA agarose bead column (Invitrogen, Carlsbad, CA, USA), which was equipped with an AKTA purifier machine. The column was extensively washed with 50 mM PBS washing buffer (pH 7.5) to remove unbound proteins. Finally, the protein was eluted with an elution buffer containing 75% 50 mM PBS and 25% 500 mM imidazole (pH 7.5). The protein was concentrated in 50 mM PBS (pH 7.5) using a 10 kDa ultrafilter (Merck Millipore, Darmstadt, Germany). Finally, the lysate and purity molecular mass of the recombinant protein were monitored using sodium dodecyl sulfate–polyacrylamide gel electrophoresis (SDS-PAGE).

Synthesis of ZIF-67@Fe₃O₄ nanoparticles

Citric acid-coated Fe₃O₄ nanoparticles were prepared according to a previously published method (Liu et al. 2009). To obtain ZIF-67@Fe₃O₄ nanoparticles, 500 mg of citric acid-coated Fe₃O₄ nanoparticles were dispersed in 10 mL of 10 mM Co(NO₃)₂·6H₂O (Aladdin Chemistry Co., Ltd. Shanghai, China) and then washed with 10 mL of deionized water. The reaction system was mechanically stirred at 1000 g and 25 °C for 1 h, after which the Co²⁺@Fe₃O₄ product was thoroughly washed with water and separated by a magnet. The Co²⁺@Fe₃O₄ nanoparticles were then re-dispersed in 10 mL of water, followed by the addition of 10 mL of 20 mM 2-MeIM (Aladdin Chemistry Co.). To obtain the ZIF-67@Fe₃O₄ nanoparticles, the mixture was mechanically stirred at 1000 g and 25 °C for 1 h. The ZIF-67@Fe₃O₄

nanoparticles were washed with methanol and water twice and then air-dried at 60 °C for 12 h.

Immobilization of AT-DAEase on ZIF-67@Fe₃O₄ nanoparticles

To prepare the AT-DAEase@ZIF-67@Fe₃O₄ nanoparticles, AT-DAEase was immobilized in the ZIF-67 shell by mixing 50 mg of ZIF-67@Fe₃O₄ nanoparticles with 1 mL of a solution containing 10 mg Co(NO₃)₂·6H₂O, 8 mg 2-methylimidazole (MeIM), and 2 mg AT-DAEase. The samples were mechanically stirred at 1000 g and 4 °C for 1 h to produce AT-DAEase@ZIF-67@Fe₃O₄. The product was washed with water and separated using a magnet. Protein concentrations were measured using the Bradford reagent (Bio-Rad, Hercules, CA, USA).

Calculation of enzyme loading

The enzyme loading (Q) of the enzyme nanoparticles was calculated (Hammes and Wu 1971) as:

$$Q = \frac{(C_0 - C)V}{m}$$

where C_0 (mg/mL) is the initial enzyme concentration without immobilization, C (mg/mL) is the final enzyme concentration of the supernatant after immobilization, m (mg) is the dry weight of ZIF-67@Fe₃O₄ nanoparticles added to the enzyme immobilization system, and V (mL) is the volume of the added enzyme solution.

Characterization of Fe₃O₄, ZIF-67@Fe₃O₄, and AT-DAEase@ZIF-67@Fe₃O₄

The magnetic nanoparticles were imaged by scanning electron microscopy (SEM) using a su1510 field emission microscope (Hitachi, Tokyo, Japan) and transmission electron microscopy (TEM) using an HT7700 electron microscope (Hitachi, Tokyo, Japan). The structural and chemical properties of the magnetic nanoparticles were also analyzed by Fourier transform infrared spectroscopy (FTIR) using a Nicolet iS50 (Thermo Fisher Scientific, Waltham, MA, USA). X-ray diffraction (XRD) patterns of nanoparticles were recorded using an X-ray diffractometer (D2 Phaser, Bruker, Germany), and the relative intensity was measured in the scattering range (2θ) of 20–60° at a step of 5° min⁻¹. Thermal gravimetric analysis (TGA) was performed using an 1100SF (Mettler, Switzerland). They were detected in the temperature range of 25–750 °C with a temperature increase at a rate of 10 °C/min under a nitrogen flow rate of 20 mL/min.

AT-DAEase activity analysis

The production of 1 μmol D-allulose within 1 min from D-fructose under some assay conditions is defined as one unit of enzyme activity. The specific activity is expressed as enzyme units per milligram of protein. In the assay, free AT-DAEase catalyzed D-fructose to D-allulose in 50 mM sodium phosphate buffer (pH 7.5) with 0.1 M Co^{2+} and without Co^{2+} . The AT-DAEase@ZIF-67@ Fe_3O_4 catalyst was in the same buffer (pH 8.0) without Co^{2+} . The bioconversion rates of D-fructose to D-allulose were determined using 50 g/L D-fructose (Aladdin Chemistry Co., Ltd.) as the substrate and 0.6 μM enzyme as the catalyst under the assay conditions of 50 °C and 55 °C for 5 min. The reaction was stopped by boiling the mixture for 10 min.

The D-allulose product and D-fructose substrate in the supernatant were detected using a high-performance liquid chromatography (HPLC) system equipped with a RID-20A refractive index detector (Shimadzu, Kyoto, Japan), an injector (Shimadzu), and a Sugar-Pak I column (Shimadzu; 30 mm \times 5 mm i.d.). The column was eluted with deionized water as the mobile phase at a flow rate of 0.4 mL/min and 85 °C. The samples (20 μL) were injected into the column. The retention times of D-fructose and D-allulose were determined using 17.02 min and 24.07 min standards, respectively.

Enzymatic characterization of free AT-DAEase and AT-DAEase@ZIF-67@ Fe_3O_4

To determine the optimal reaction temperature, the activities of free AT-DAEase and AT-DAEase@ZIF-67@ Fe_3O_4 were measured at temperatures ranging from 45–70 °C. The mixed samples were incubated for 5 min and activity was determined. The thermal stability of free AT-DAEase and AT-DAEase@ZIF-67@ Fe_3O_4 was characterized by incubating the enzyme mixture at 55 °C in 50 mM sodium phosphate buffer (pH 7.5). The mixture was sampled at 0, 20, 40, 60, 80, 100, 120, 240, and 360 min, and the residual enzyme activities of the samples were also measured. The effect of pH on the enzyme activities of AT-DAEase@ZIF-67@ Fe_3O_4 was determined by incubating the reaction mixture of 50 mM sodium phosphate buffer with 50 g/L D-fructose in the pH range of 7.0–9.0. The mixtures were incubated at 55 °C and pH 7.0, 7.5, 8.0, 8.5, and 9.0, respectively, for 5 min, and then the activities were measured.

The kinetic analyses were implemented in 50 mM sodium phosphate buffer containing D-fructose at different concentrations ranging from 0.025 to 18 mM. The free enzyme's reaction was at pH 7.5 and 50 °C, and the AT-DAEase@ZIF-67@ Fe_3O_4 's reaction was at pH 8.0 and 55 °C. All experiments of enzymic reactions were performed in triplicate. The values of apparent

Michaelis–Menten constant K_m , the maximal reaction rate (V_{max}) and catalytic number (K_{cat}) were calculated using the substrate saturation plotting according to the Michaelis–Menten equation (Matyska and Kovár 1985).

Reusability assay of AT-DAEase@ZIF-67@ Fe_3O_4

The reusability of AT-DAEase@ZIF-67@ Fe_3O_4 was determined by incubating the mixture with the immobilized enzyme and 50 g/L D-fructose dissolved in 50 mM sodium phosphate buffer (pH 8.0) at 55 °C for 5 min. After the reaction, the immobilized enzyme was separated by a magnet, and the AT-DAEase@ZIF-67@ Fe_3O_4 particles were washed three times with sodium phosphate buffer and reused for the next cycle. This procedure was repeated eight times. The reusability of AT-DAEase@ZIF-67@ Fe_3O_4 was analyzed through the activity of AT-DAEase@ZIF-67@ Fe_3O_4 after every cycle. The amounts of D-fructose and D-allulose were analyzed using HPLC after the reaction was over.

Results

Expression, purification and characterization of AT-DAEase

We inserted the DNA fragment encoding AT-DAEase into the 6 \times His-tagged vector pRSFDuet-1 to construct the plasmid pRSF-DAE to express AT-DAEase. We transformed the plasmid pRSF-DAE into *E. coli* BL21 (DE3) to obtain the recombinant strain and cultured it for expression. After induction with IPTG at 18 °C and SDS-PAGE analysis, the soluble AT-DAEase protein was identified in the supernatant of the cell lysate of the recombinant *E. coli* following centrifugation (Fig. 1A, lane a). To verify and characterize the enzyme, it was purified using the AKTA system. SDS-PAGE revealed a band of purified protein with an approximate molecular mass of 32 kDa, representing AT-DAEase subunits (Fig. 1A, lane b).

A catalysis experiment was performed using purified free AT-DAEase. The bioconversion ratio reached approximately 32% under the optimal conditions of 50 °C and pH 7.5 (Fig. 1B), as previously reported (Kim et al. 2006b, a). The bioconversion ratio was approximately 35% higher when Co^{2+} was present in the reaction system than that without Co^{2+} . The specific activities of free AT-DAEase reached approximately 55 U mg^{-1} and 63 U mg^{-1} when the reaction system did not contain Co^{2+} and with 0.1 M Co^{2+} , respectively.

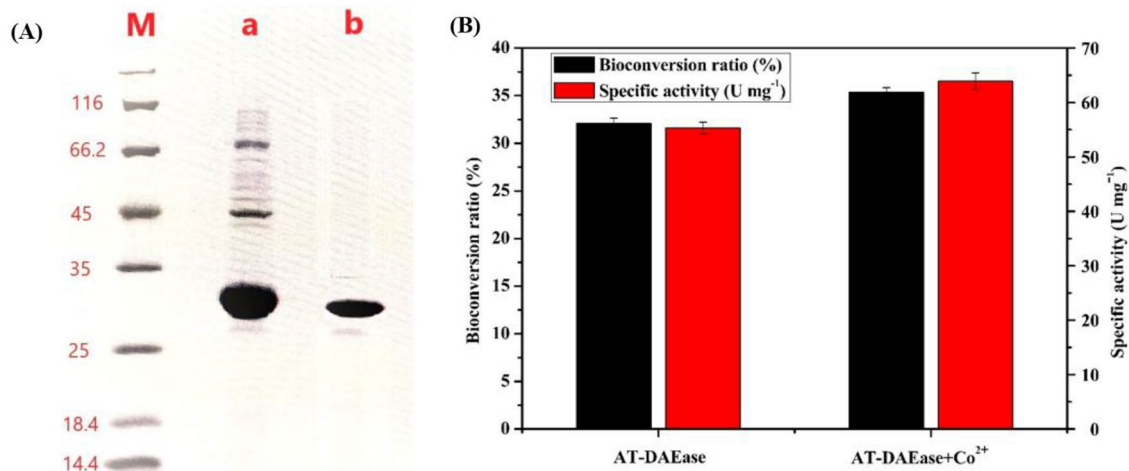


Fig. 1 Characterization of AT-DAEase. **A** SDS-PAGE of the expressed proteins. Lane M contains the molecular size markers; lane a is the crude lysate of AT-DAEase, and lane b is the purified 32 kDa

AT-DAEase. **B** The bioconversion ratio and specific activities of AT-DAEase in the absence and presence of Co²⁺ in the reaction system

Design strategy of immobilizing AT-DAEase into ZIF-67@Fe₃O₄

The design strategy for immobilizing AT-DAEase into ZIF-67@Fe₃O₄ is shown in Fig. 2. We obtained the enzyme AT-DAEase from the recombinant *E. coli* BL21 (DE3) strain after expression and purification. Citric acid-coated magnetic Fe₃O₄ nanoparticles were prepared using a solvothermal reaction, including the reduction of FeCl₃ by trisodium citrate in ethylene glycol. We chose ZIF-67 to immobilize DAEase because of its different pore sizes, high surface area, transition metal Co, and rich N resources (Kaneti et al. 2017). These properties of ZIF-67

could potentially improve the thermal stability of DAEase and provide the essential metal iron Co²⁺, which plays a crucial role in DAEase catalysis by anchoring the substrate. Furthermore, using ZIF-67 to immobilize DAEase facilitated the formation of chemical bonds between Co²⁺ and the enzyme, and simplified the process of preparation of the reaction system and purification of the product. Therefore, citric acid-coated Fe₃O₄ nanoparticles were self-assembled with Co(NO₃)₂·6H₂O and 2-MeIM individually to generate ZIF-67@Fe₃O₄ nanoparticles. Finally, we encapsulated the enzyme AT-DAEase into the ZIF-67@Fe₃O₄ nanoparticles by fixing the ZIF-67 shell, Co(NO₃)₂·6H₂O, and 2-MeIM.

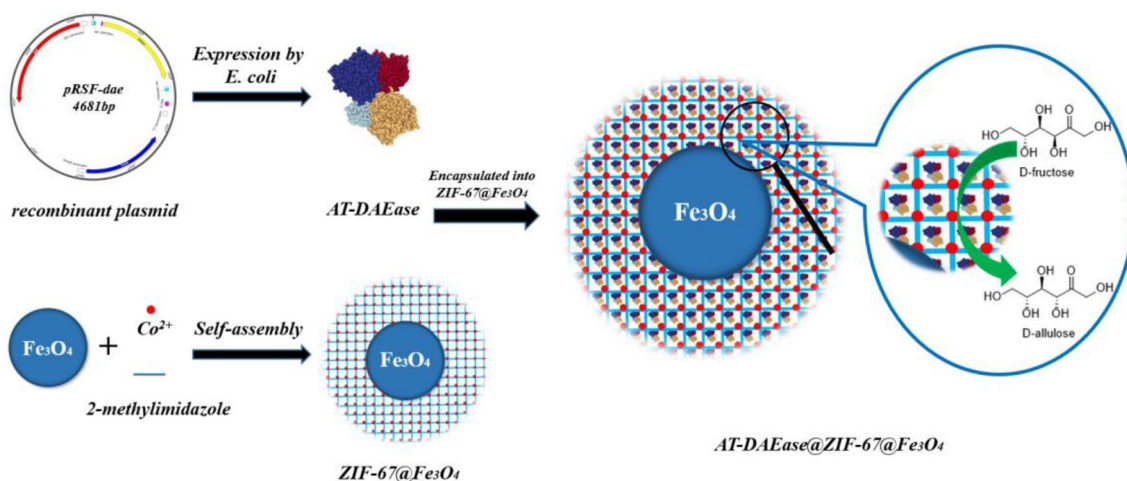


Fig. 2 Immobilization of AT-DAEase into ZIF-67@Fe₃O₄. The figure presents a schematic diagram of the production of ZIF-67@Fe₃O₄ immobilized AT-DAEase

Characterization of Fe_3O_4 , $\text{ZIF-67@Fe}_3\text{O}_4$ and $\text{AT-DAEase@ZIF-67@Fe}_3\text{O}_4$

To characterize the sizes and shapes of Fe_3O_4 , $\text{ZIF-67@Fe}_3\text{O}_4$ and $\text{AT-DAEase@ZIF-67@Fe}_3\text{O}_4$ nanoparticles, they were imaged using SEM and TEM. We counted the sizes of the magnetite particles according to the SEM and TEM images. The size range of the diameter of the prepared spherical Fe_3O_4 magnetic nanoparticles was 80–260 nm, and their average diameter was about 200 nm (Fig. 3A, D). As shown in Fig. 3A, B, D and E, both the Fe_3O_4 nanoparticles and $\text{ZIF-67@Fe}_3\text{O}_4$ nanoparticles showed the spherical shapes, and exhibited well dispersed. The surfaces of Fe_3O_4 nanoparticles were smooth, but they became slightly crude after coating the ZIF-67 material. The SEM images in Fig. 3A, B demonstrated that the particle sizes of $\text{ZIF-67@Fe}_3\text{O}_4$ nanoparticles were significantly higher than those of the Fe_3O_4 nanoparticles. The comparison of the particle sizes and shapes between Fe_3O_4 nanoparticles and $\text{ZIF-67@Fe}_3\text{O}_4$

Fe_3O_4 nanoparticles revealed that co-precipitation successfully generated a ZIF-67 shell with an average thickness of about 20 nm on the surface of the Fe_3O_4 nanoparticles (Fig. 3D, E). The SEM image (Fig. 3C) and TEM image (Fig. 3F) showed that the $\text{AT-DAEase@ZIF-67@Fe}_3\text{O}_4$ nanoparticles exhibited particularly rough surfaces and a particle agglomeration. The TEM images of $\text{ZIF-67@Fe}_3\text{O}_4$ nanoparticles (Fig. 3E) and $\text{AT-DAEase@ZIF-67@Fe}_3\text{O}_4$ nanoparticles (Fig. 3F) revealed the formation of MOF shells with an average thickness of about 50 nm via the aggregation of ZIF-67 nanoparticles with encapsulated enzymes. Therefore, the characterization of Fe_3O_4 , $\text{ZIF-67@Fe}_3\text{O}_4$ and $\text{AT-DAEase@ZIF-67@Fe}_3\text{O}_4$ showed the successful creation of MOF nanoparticle aggregates and the changes in the shapes and sizes of the $\text{AT-DAEase@ZIF-67@Fe}_3\text{O}_4$ nanoparticles.

To confirm the attachment of the MOF and the enzyme, FTIR spectral analysis was performed. Figure 4A shows the comparative spectral analysis of Fe_3O_4 , $\text{ZIF-67@Fe}_3\text{O}_4$, and $\text{AT-DAEase@ZIF-67@Fe}_3\text{O}_4$. The absorption

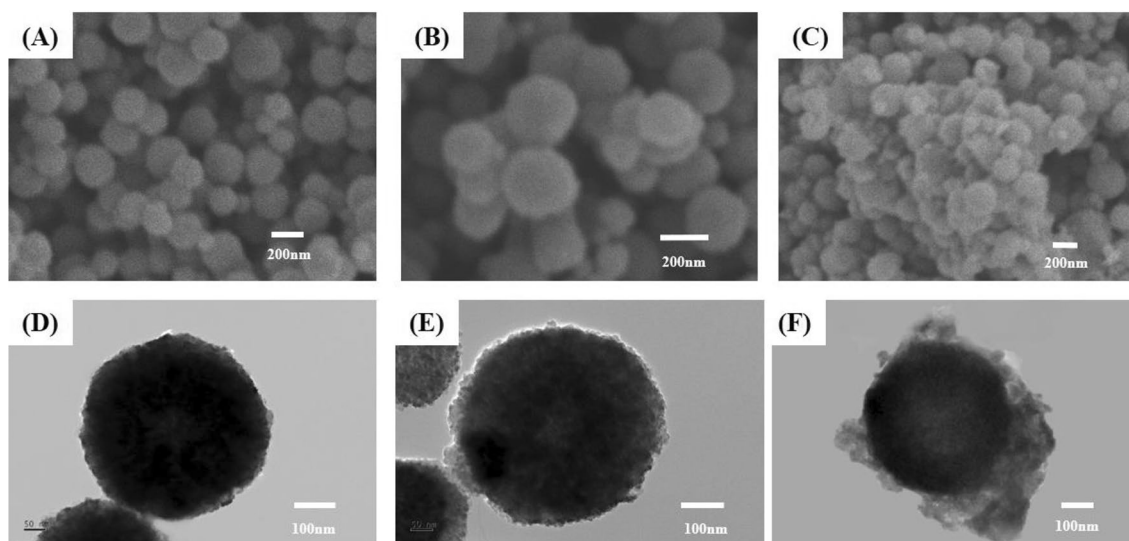


Fig. 3 SEM images of **A** Fe_3O_4 , **B** $\text{ZIF-67@Fe}_3\text{O}_4$, and **C** $\text{AT-DAEase@ZIF-67@Fe}_3\text{O}_4$. TEM images of **D** Fe_3O_4 , **E** $\text{ZIF-67@Fe}_3\text{O}_4$, and **F** $\text{AT-DAEase@ZIF-67@Fe}_3\text{O}_4$

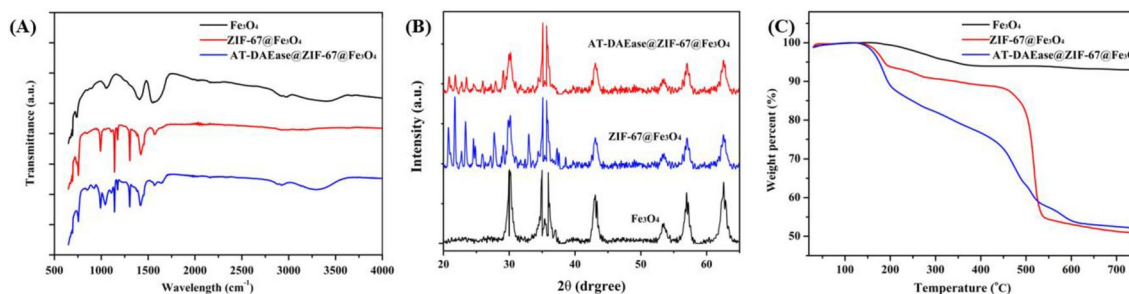


Fig. 4 **A** Fourier transforms infrared spectra, **B** XRD patterns and **C** thermal gravimetric analysis of Fe_3O_4 , $\text{ZIF-67@Fe}_3\text{O}_4$ and $\text{AT-DAEase@ZIF-67@Fe}_3\text{O}_4$

band centered at 1610 cm^{-1} in the sample Fe_3O_4 (black line) represents the C=O stretching vibrations of the citric acid groups coating on Fe_3O_4 . The peak centered at 582 cm^{-1} indicated the Fe–O stretching. Comparison of Fe_3O_4 with $\text{ZIF-67@Fe}_3\text{O}_4$ revealed that the bands in the range of $600\text{--}1500\text{ cm}^{-1}$ were attributed to the characteristic stretching and bending modes of the imidazole ring of 2-MeIM. The FTIR spectrum of AT-DAE@ZIF-67@ Fe_3O_4 displayed two absorption bands at 1635 and 3250 cm^{-1} compared to that of $\text{ZIF-67@Fe}_3\text{O}_4$. As shown in Fig. 4B, the XRD patterns illustrated the characteristic peaks of Fe_3O_4 are completely consistent with those previously reported (Liu et al. 2009). Compared to the spectrums of Fe_3O_4 and $\text{ZIF-67@Fe}_3\text{O}_4$, significant new peaks generated at the interval of $20\text{--}30$ after ZIF-67 was attached. Also, the spectrum of AT-DAE@ZIF-67@ Fe_3O_4 nanoparticles had the characteristic peaks of Fe_3O_4 and ZIF-67 materials.

To further confirm the attachment of the MOF material and the enzyme, TGA plots were also obtained. They revealed that the magnetic Fe_3O_4 nanoparticles lost 7.1% of their weight in the range of $150\text{--}370\text{ }^\circ\text{C}$, corresponding to the removal of water and citric acid functionalities (Fig. 4B). The $\text{ZIF-67@Fe}_3\text{O}_4$ nanoparticles lost an initial weight of approximately 6% within the range of $150\text{--}200\text{ }^\circ\text{C}$, which was related to the removal of guest water molecules. The second weight loss of about 5% was observed between 200 and $450\text{ }^\circ\text{C}$ due to the loss of unreacted ligands in the pores and citric acid functionalities in the Fe_3O_4 material. The third weight loss of 38% was observed between 450 and $550\text{ }^\circ\text{C}$ due to the decomposition of ZIF-67. The residual 51% of the weight was cobalt and iron. For AT-DAE@ZIF-67@ Fe_3O_4 nanoparticles, the curve showed an initial weight loss of approximately 12% that was related to the removal of the guest molecules, including enzymes, at temperatures ranging from 150 to $260\text{ }^\circ\text{C}$. In the range of $250\text{--}450\text{ }^\circ\text{C}$, AT-DAE@ZIF-67@ Fe_3O_4 exhibited a supernumerary 16% weight loss compared with the Fe_3O_4 sample and $\text{ZIF-67@Fe}_3\text{O}_4$ sample. We speculated the 16% weight loss was resulted from the attached enzyme of the prepared MOF samples. During the temperature of 450 and $550\text{ }^\circ\text{C}$, the residual enzyme molecules and ZIF-67 might be decomposed.

AT-DAE enzyme load and specific activity detection

The enzyme loading and specific activities are summarized in Table 1. The enzyme loading was 37 mg enzyme per gram of Fe_3O_4 nanoparticles, which was consistent with the TGA results. The AT-DAE@ZIF-67@ Fe_3O_4 nanoparticles showed the highest activity of 65.1 U mg^{-1} , which was 18% higher than that of free AT-DAE. To detect the bioconversion rate of D-fructose to D-allulose by AT-DAE@ZIF-67@ Fe_3O_4 , we performed an epimerization reaction using the free enzymes AT-DAE and AT-DAE@ZIF-67@ Fe_3O_4 under optimal reaction conditions (pH 8.0 and temperature of $55\text{ }^\circ\text{C}$). The free AT-DAE showed a higher bioconversion ratio of 35.4% when Co^{2+} was added to the reaction mixture than that without Co^{2+} . AT-DAE@ZIF-67@ Fe_3O_4 had a higher bioconversion ratio than the free AT-DAE with or without Co^{2+} in the reaction mixture. At equilibrium, the bioconversion ratio of D-fructose to D-allulose was 38.1%, which was 18.6% higher than that of AT-DAE without Co^{2+} .

Enzymatic properties of MOF-immobilized AT-DAE@ZIF-67@ Fe_3O_4

Thermal stability is an essential requirement for industrial enzymes because the reaction at higher temperatures can increase the bioconversion rate and reactant solubility, and reduce the risk of contamination during bio-catalytic processes. To study the thermal stability of the MOF-immobilized AT-DAE@ZIF-67@ Fe_3O_4 , we measured the relative enzyme activities of the temperature profile from 45 to $70\text{ }^\circ\text{C}$ with D-fructose as a substrate. AT-DAE@ZIF-67@ Fe_3O_4 exhibited a higher level of activity than free AT-DAE over the entire temperature range (Fig. 5A). The maximum activities of free AT-DAE and AT-DAE@ZIF-67@ Fe_3O_4 were observed at $50\text{ }^\circ\text{C}$ and $55\text{ }^\circ\text{C}$, respectively, indicating that immobilization increased the optimal temperature of free AT-DAE. The enzyme activity of almost all the reactions of AT-DAE@ZIF-67@ Fe_3O_4 surpassed 80% at temperatures from $45\text{ }^\circ\text{C}$ to $70\text{ }^\circ\text{C}$, while that of only the optimal temperature reaction of free AT-DAE was comparable (Fig. 5A). We also detected the residual activities of free AT-DAE and AT-DAE@ZIF-67@

Table 1 Bioconversion ratio, specific activities and enzyme loading capacities of free AT-DAE, free AT-DAE + Co^{2+} and AT-DAE@ZIF-67@ Fe_3O_4

	Bioconversion ratio (%)	Specific activity (U mg^{-1})	Enzyme loading capacity (mg per g Fe_3O_4)
Free AT-DAE	32.1	55.3	–
Free AT-DAE + Co^{2+}	35.4	63.9	–
AT-DAE@ZIF-67@ Fe_3O_4	38.1	65.1	37

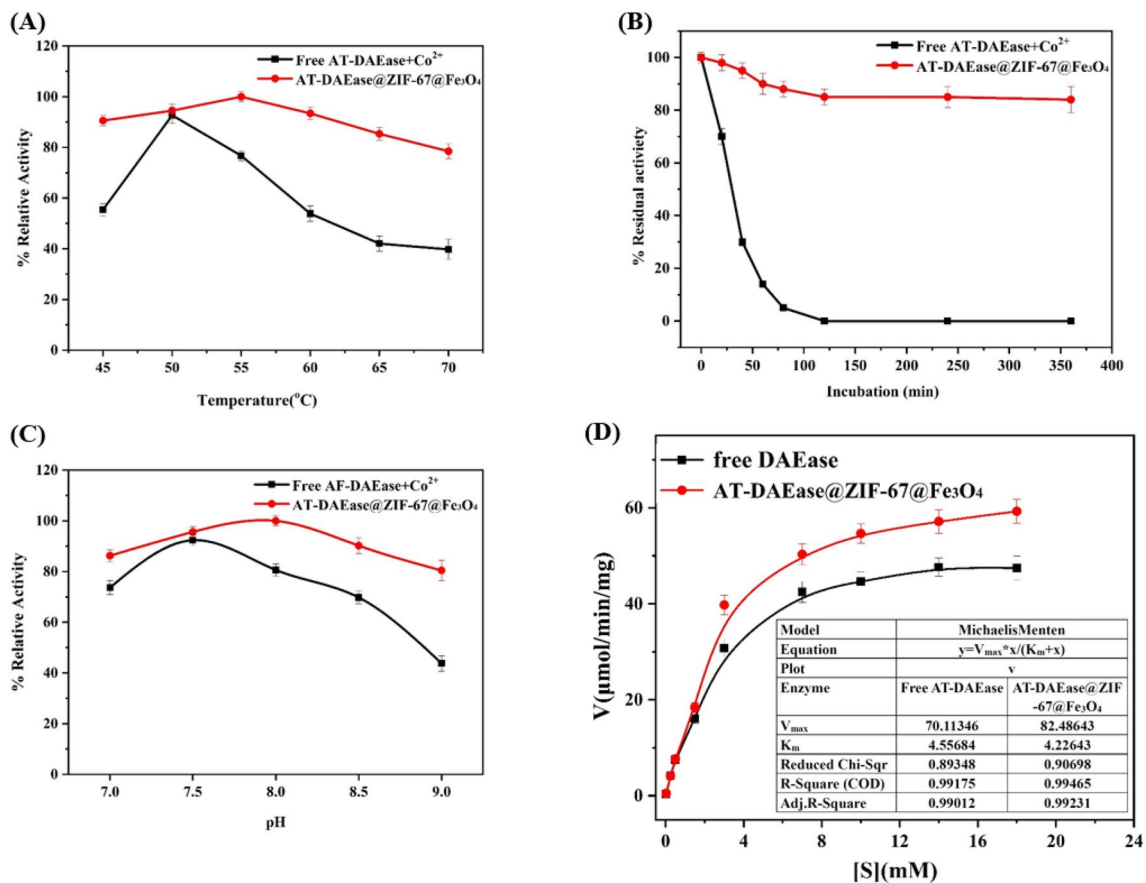


Fig. 5 Reaction properties of free AT-DAEase and AT-DAEase@ZIF-67@Fe₃O₄. **A** Relative activities at different temperatures. **B** Relative activities at 55 °C during the time of 60 to 360 min. **C** Relative activity at different pH values. **D** Michaelis–Menten kinetic curve

Fe₃O₄ reacting at 55 °C from 60 to 360 min. The residual activity of AT-DAEase@ZIF-67@Fe₃O₄ remained above 80% after 360 min, while it decreased to almost zero after 120 min in the free AT-DAEase reaction system (Fig. 5B). These results indicate that the thermal stability of the MOF-immobilized AT-DAEase@ZIF-67@Fe₃O₄ was better than that of the free AT-DAEase.

pH stability is another key factor affecting the enzyme activity of AT-DAEase, and is an important operational factor for industrial enzymes. To investigate the effect of pH on the conversion of D-fructose to D-allulose, we measured the activity of free AT-DAEase and AT-DAEase@ZIF-67@Fe₃O₄ at pH values of 7.0, 7.5, 8.0, 8.5, and 9.0. The optimum pH was 7.5 for free AT-DAEase and 8.0 for AT-DAEase@ZIF-67@Fe₃O₄ (Fig. 5C). In general, AT-DAEase@ZIF-67@Fe₃O₄ activities over the pH range were higher than activities of the free AT-DAEase. AT-DAEase@ZIF-67@Fe₃O₄ retained > 80% activity at pH 7.0–9.0, while free AT-DAEase displayed < 70% activity, except at pH 7.5. The findings indicate the significant advantage of AT-DAEase@ZIF-67@Fe₃O₄ over the free AT-DAEase in pH stability of the enzyme.

To further evaluate the enzymatic properties of AT-DAEase@ZIF-67@Fe₃O₄, we calculated the kinetic values according to the classical Michaelis equation using D-fructose as substrate, and compared them with those of the free AT-DAEase. As shown in Fig. 5D, the K_m of AT-DAEase@ZIF-67@Fe₃O₄ was 4.2 mM, 8.7% lower than that of the free AT-DAEase. The V_{max} and K_{cat} of AT-DAEase@ZIF-67@Fe₃O₄ were 82.5 μmol min⁻¹ mg⁻¹ and 44.0 s⁻¹, respectively 17.7% and 17.8% higher than those of the free enzymes. These suggested that AT-DAEase@ZIF-67@Fe₃O₄ had a higher substrate affinity toward D-fructose and a higher reaction rate.

Reusability of AT-DAEase@ZIF-67@Fe₃O₄

To reduce the cost of production in bio-catalytic processes for industrial applications, the immobilized enzymes are always recycled. This is a key reason favoring the use of immobilized enzymes in industrial applications. The immobilized enzyme was recycled through magnetic absorption for next cycle usage, and this process only took 30 s to completely recover the particles in the solution (Fig. 6A).

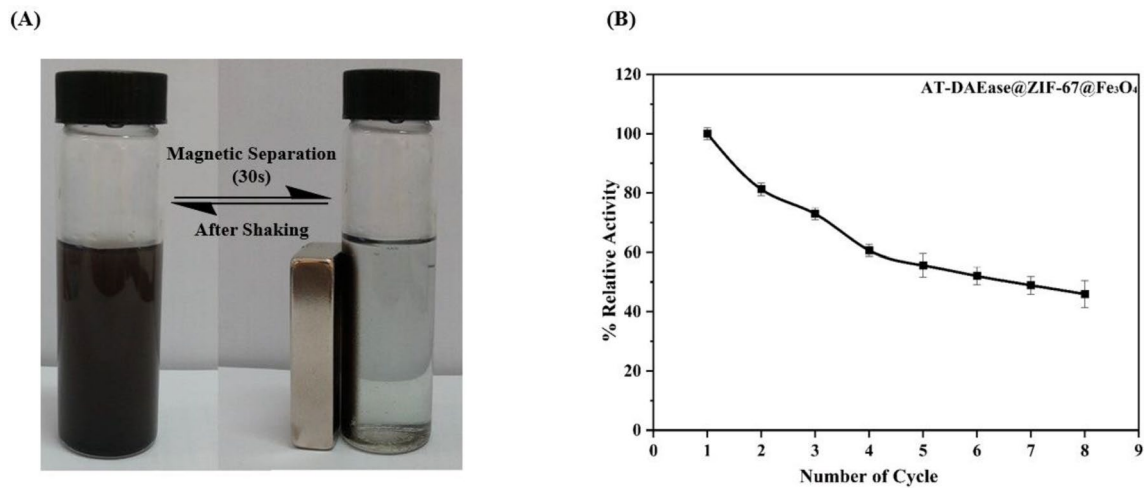


Fig. 6 **A** The magnetic separation behavior of AT-DAEase@ZIF-67@Fe₃O₄. **B** Relative activities of AT-DAEase@ZIF-67@Fe₃O₄ after eight cycles of use

To evaluate the feasibility of recovery and recycling of AT-DAEase@ZIF-67@Fe₃O₄, the relative activities were determined during eight consecutive rounds of the bioconversion of D-fructose to D-allulose at pH 8.0 and 55 °C. AT-DAEase@ZIF-67@Fe₃O₄ retained > 45% of its initial activity after eight cycles of enzyme use (Fig. 6B).

Discussion

In the present study, AT-DAEase was successfully encapsulated into the ZIF-67@Fe₃O₄ magnetic hybrid MOF using a self-assembly strategy. A prior study described the immobilization of D-allulose 3-epimerase from *C. cellulolyticum* on artificial oil bodies with the aim of decreasing the cost of D-allulose production (Tseng et al. 2014). In contrast, we anchored Co on MOF ZIF67 to facilitate the catalytic reaction of the Co-dependent enzyme AT-DAEase, with magnetic Fe₃O₄ as the carrier of the catalyst. This design omitted the addition of Co to the reaction system and simplified the separation of the catalyst and its recycling. SEM and TEM imaging clearly demonstrated the changes in the shapes and sizes of the AT-DAEase@ZIF-67@Fe₃O₄ nanoparticles. In the FTIR spectral analysis, the two bands at 1635 and 3250 cm⁻¹ were attributed to the C=O stretching vibration and N–H stretching vibration of the amide group, respectively, confirming that AT-DAEase was immobilized on ZIF-67@Fe₃O₄. XRD results indicated that ZIF-67 was coated on the surface of Fe₃O₄ in a certain crystal form. TGA plot analysis demonstrated a weight loss that was generally consistent with the removal of all molecules at temperatures ranging from 25 to 750 °C. The weight percentage of AT-DAEase was approximately 5% in ZIF-67. The FTIR

spectral analysis and TGA plots confirmed the successful formation of the ZIF-67@Fe₃O₄ core–shell structures.

AT-DAEase@ZIF-67@Fe₃O₄ displayed high catalytic activity for D-fructose to D-allulose, and its specific activity reached to 65.1 U mg⁻¹. The higher bioconversion ratio of AT-DAEase@ZIF-67@Fe₃O₄ than that of free AT-DAEase suggests that the ZIF-67@Fe₃O₄ MOF improves the bioconversion efficiency of the AT-DAEase enzyme. The synthesized AT-DAEase@ZIF-67@Fe₃O₄ displayed a significant improvement in thermal stability compared to the free enzyme AT-DAEase. This indicated that the MOF material enabled the enzyme to resist high temperatures. The collective results suggest that adding Co²⁺ to the reaction mixture can increase the bioconversion rate, consistent with previous reports (Kim et al. 2006a, b; Tseng et al. 2014). In addition, AT-DPEase@ZIF-67@Fe₃O₄ displayed an improved bioconversion efficiency compared to that of free AT-DPEase with Co²⁺. The increased thermal stability of the immobilized AT-DPEase may have led to an improvement in the bioconversion efficiency. The optimal conditions for maximum enzyme activity of AT-DAEase@ZIF-67@Fe₃O₄ were 55 °C and pH 8.0. The optimal temperature and pH of free AT-DAEase were 50 °C and 7.5, respectively. The improved optimal temperature should benefit from modification of the MOF material. The mechanism of the optimal pH property shifting is unclear. The residual activity remained above 80% of the maximum activity at high temperatures ranging from 55–70 °C and a pH range of 7.0–9.0. These results are consistent with those of previous studies reporting that the MOF coating could protect enzymes from adverse conditions and enhance their stability (Tseng et al. 2014; Pei et al. 2020). When AT-DAEase was immobilized with graphene oxide, the optimal pH was 7.5, the optimal temperature was 60 °C, and the biotransformation ratio reached 40%, but the enzyme

activity after eight cycles of use remained at approximately 25% (Dedania et al. 2017). In the present study, AT-DAEase@ZIF-67@Fe₃O₄ could be reused for eight cycles with enzyme activity remaining at > 45% of its initial activity. Therefore, our enzyme modification method appears to be more suitable for recycling.

The enzymatic properties of MOF-immobilized AT-DAEase@ZIF-67@Fe₃O₄ illustrated that the ZIF-67@Fe₃O₄ material could efficiently protect the AT-DAEase enzyme to enhance its thermal stability and the porous structure also facilitated the transportation of the substrate and product. Moreover, AT-DAEase@ZIF-67@Fe₃O₄ had a slightly higher bioconversion rate than that of the free enzyme AT-DAEase, which may be related to the increases in optimal temperature and pH. AT-DAEase@ZIF-67@Fe₃O₄ exhibited a higher substrate affinity toward D-fructose and a higher reaction rate, possibly due to the microenvironments of ZIF-67@Fe₃O₄ crystals. The magnetic ZIF-67 scaffold could enable the separation of the enzyme from the reaction system using a magnet, facilitating the reuse of the catalyst (Talekar et al. 2012; Zdarta et al. 2018). In the present study, AT-DAEase@ZIF-67@Fe₃O₄ could be reused multiple times if used under optimal conditions. Therefore, immobilization of the enzyme could reduce the often high cost of industrial applications of enzymes. ZIF-67@Fe₃O₄-immobilized AT-DAEase has potential applications in the production of D-allulose at a lower cost than the free enzyme. Therefore, the Co-based magnetic hybrid ZIF-67@Fe₃O₄ is a suitable host matrix for immobilizing Co-dependent AT-DAEase for the large-scale industrial preparation of D-allulose.

Funding This work was supported by the Natural Science Foundation of Jiangsu Province (BK20190610) and the 111 Project (111-2-06).

Data availability All data generated or analyzed during this study are included in this published article.

Declarations

Conflict of interest All authors declare that they have no conflict of interest.

Ethical approval This article does not contain any studies with human participants performed by any of the authors.

References

Dedania SR, Patel MJ, Patel DM, Akhiani RC, Patel DH (2017) Immobilization on graphene oxide improves the thermal stability and bioconversion efficiency of D-psicose 3-epimerase for rare sugar production. *Enzyme Microb Technol* 107:49–56. <https://doi.org/10.1016/j.enzmictec.2017.08.003>

- Dicosimo R, McAuliffe JC, Poulou AJ, Bohlmann G (2013) Industrial use of immobilized enzymes. *Chem Soc Rev* 42(15):6437–6474. <https://doi.org/10.1039/C3CS35506C>
- Franssen MC, Steunenberg P, Scott EL, Zuilhof H, Sanders JP (2013) Immobilised enzymes in biorenewables production. *Chem Soc Rev* 42(15):6491–6533. <https://doi.org/10.1039/C3CS00004D>
- Hammes GG, Wu CW (1971) Regulation of enzyme activity. The activity of enzymes can be controlled by a multiplicity of conformational equilibria. *Science* 172(3989):1205–1211. <https://doi.org/10.1126/science.172.3989.1205>
- Itoh H, Okaya H, Khan AR, Tajima S, Hayakawa S, Izumori K (1994) Purification and characterization of D-tagatose 3-epimerase from *Pseudomonas* sp. ST-24. *Biosci Biotech Bioch* 58(12):2168–2171. <https://doi.org/10.1271/bbb.58.2168>
- Kaneti YV, Dutta S, Hossain MSA, Shiddiky MJA, Tung KL, Shieh FK, Tsung CK, Wu KC, Yamauchi Y (2017) Strategies for improving the functionality of zeolitic imidazolate frameworks: tailoring nanoarchitectures for functional applications. *Adv Mater* 29(38):1700213. <https://doi.org/10.1002/adma.20170213>
- Kim K, Kim HJ, Oh DK, Cha SS, Rhee S (2006a) Crystal structure of D-psicose 3-epimerase from *Agrobacterium tumefaciens* and its complex with true substrate D-fructose: a pivotal role of metal in catalysis, an active site for the non-phosphorylated substrate, and its conformational changes. *J Mol Biol* 361(5):920–931. <https://doi.org/10.1016/j.jmb.2006.06.069>
- Kim HJ, Hyun EK, Kim YS, Lee YJ, Oh DK (2006b) Characterization of an *Agrobacterium tumefaciens* D-psicose 3-epimerase that converts D-fructose to D-psicose. *Appl Environ Microbiol* 72(2):981–985. <https://doi.org/10.1128/AEM.72.2.981-985.2006>
- Li P, Moon SY, Guelta MA, Harvey SP, Hupp JT, Farha OK (2016) Encapsulation of a nerve agent detoxifying enzyme by a mesoporous zirconium metal-organic framework engenders thermal and long-term stability. *J Am Chem Soc* 138(26):8052–8055. <https://doi.org/10.1021/jacs.6b03673>
- Lian X, Fang Y, Joseph E, Wang Q, Li J, Banerjee S, Lollar C, Wang X, Zhou HC (2017) Enzyme-MOF (metal-organic framework) composites. *Chem Soc Rev* 46(11):3386–3401. <https://doi.org/10.1039/C7CS00058H>
- Liang K, Ricco R, Doherty CM, Styles MJ, Bell S, Kirby N, Mudie S, Haylock D, Hill AJ, Doonan CJ, Falcaro P (2015) Biomimetic mineralization of metal-organic frameworks as protective coatings for biomacromolecules. *Nat Commun* 6:7240. <https://doi.org/10.1038/ncomms8240>
- Lim B, Kim H, Oh D (2009) A stable immobilized D-psicose 3-epimerase for the production of D-psicose in the presence of borate. *Process Biochem* 44(8):822–828. <https://doi.org/10.1016/j.procbio.2009.03.017>
- Liu J, Sun Z, Deng Y, Zou Y, Li C, Guo X, Xiong L, Gao Y, Li F, Zhao D (2009) Highly water-dispersible biocompatible magnetite particles with low cytotoxicity stabilized by citrate groups. *Angew Chem Int Ed Engl* 48(32):5875–5879. <https://doi.org/10.1002/anie.200901566>
- Mao S, Cheng X, Zhu Z, Chen Y, Li C, Zhu M, Liu X, Lu F, Qin HM (2020) Engineering a thermostable version of D-allulose 3-epimerase from *Rhodospirellula baltica* via site-directed mutagenesis based on B-factors analysis. *Enzyme Microb Technol* 132:109441. <https://doi.org/10.1016/j.enzmictec.2019.109441>
- Matsuo T, Suzuki H, Hashiguchi M, Izumori K (2002) D-psicose is a rare sugar that provides no energy to growing rats. *J Nutr Sci Vitaminol* 48(1):77–80. <https://doi.org/10.3177/jnsv.48.77>
- Matyska L, Kovár J (1985) Comparison of several non-linear-regression methods for fitting the Michaelis-Menten equation. *Biochem J* 231(1):171–177
- Meshkat S, Kaliaguine S, Rodrigue D (2020) Comparison between ZIF-67 and ZIF-8 in Pebax® MH-1657 mixed matrix membranes

- for CO₂ separation. *Sep Purif Technol* 235:116150–116150. <https://doi.org/10.1016/j.seppur.2019.116150>
- Mu W, Chu F, Xing Q, Yu S, Zhou L, Jiang B (2011) Cloning, expression, and characterization of a D-psicose 3-epimerase from *Clostridium cellulolyticum* H10. *J Agric Food Chem* 59(14):7785–7792. <https://doi.org/10.1021/jf201356q>
- Patel SN, Singh V, Sharma M, Sangwan RS, Singhal NK, Singh SP (2018) Development of a thermo-stable and recyclable magnetic nanobiocatalyst for bioprocessing of fruit processing residues and D-allulose synthesis. *Bioresour Technol* 247:633–639. <https://doi.org/10.1016/j.biortech.2017.09.112>
- Patel SN, Kaushal G, Singh SP (2020) A novel D-allulose 3-epimerase gene from the metagenome of a thermal aquatic habitat and D-allulose production by bacillus subtilis whole-cell catalysis. *Appl Environ Microbiol* 86(5):e02605-e2619. <https://doi.org/10.1128/AEM.02605-19>
- Patel SN, Kaushal G, Singh SP (2021) D-allulose 3-epimerase of *Bacillus* sp. origin manifests profuse heat-stability and noteworthy potential of D-fructose epimerization. *Microb Cell Fact* 20(1):60. <https://doi.org/10.1186/s12934-021-01550-1>
- Pei X, Zhang H, Meng L, Xu G, Yang L, Wu J (2013) Efficient cloning and expression of a thermostable nitrile hydratase in *Escherichia coli* using an auto-induction fed-batch strategy. *Process Biochem* 48(12):1921–1927. <https://doi.org/10.1016/j.procbio.2013.09.004>
- Pei X, Wu Y, Wang J, Chen Z, Liu W, Su W, Liu F (2020) Biomimetic mineralization of nitrile hydratase into a mesoporous cobalt-based metal-organic framework for efficient biocatalysis. *Nanoscale* 12(2):967–972. <https://doi.org/10.1039/c9nr06470b>
- Sheldon RA, Woodley JM (2018) Role of biocatalysis in sustainable chemistry. *Chem Rev* 118(2):801–838. <https://doi.org/10.1021/acs.chemrev.7b00203>
- Sun Y, Hayakawa S, Ogawa M, Fukada K, Izumori K (2008) Influence of a rare sugar, D-psicose, on the physicochemical and functional properties of an aerated food system containing egg albumen. *J Agric Food Chem* 56(12):4789–4796. <https://doi.org/10.1021/jf800050d>
- Talekar S, Ghodake V, Ghotage T, Rathod P, Deshmukh P, Nadar S, Mulla M, Ladole M (2012) Novel magnetic cross-linked enzyme aggregates (magnetic CLEAs) of alpha amylase. *Bioresour Technol* 123:542–547. <https://doi.org/10.1016/j.biortech.2012.07.044>
- Tseng CW, Liao CY, Sun Y, Peng CC, Tzen JT, Guo RT, Liu JR (2014) Immobilization of *Clostridium cellulolyticum* D-psicose 3-epimerase on artificial oil bodies. *J Agric Food Chem* 62(28):6771–6776. <https://doi.org/10.1021/jf502022w>
- Wu X, Yang C, Ge J, Liu Z (2015) Polydopamine tethered enzyme/metal-organic framework composites with high stability and reusability. *Nanoscale* 7(45):18883–18886. <https://doi.org/10.1039/c5nr05190h>
- Yogapriya R, Datta KKR (2020) Porous fluorinated graphene and ZIF-67 composites with hydrophobic-oleophilic properties towards oil and organic solvent sorption. *J Nanosci Nanotechnol* 20(5):2930–2938. <https://doi.org/10.1166/jnn.2020.17465>
- Zdarta J, Meyer A, Jesionowski T, Pinelo M (2018) A general overview of support materials for enzyme immobilization: characteristics, properties, practical utility. *Catalysts* 8(2):92. <https://doi.org/10.3390/catal8020092>
- Zhang W, Fang D, Xing Q, Zhou L, Jiang B, Mu W (2013) Characterization of a novel metal-dependent D-psicose 3-epimerase from *Clostridium scindens* 35704. *PLoS ONE* 8(4):e62987. <https://doi.org/10.1371/journal.pone.0062987>
- Zheng L, Sun Y, Wang J, Huang H, Geng X, Tong Y, Wang Z (2018) Preparation of a flower-like immobilized D-psicose 3-epimerase with enhanced catalytic performance. *Catalysts* 8(10):468. <https://doi.org/10.3390/catal8100468>
- Zhu Y, Men Y, Bai W, Li X, Zhang L, Sun Y, Ma Y (2012) Overexpression of D-psicose 3-epimerase from *Ruminococcus* sp. in *Escherichia coli* and its potential application in D-psicose production. *Biotechnol Lett* 34(10):1901–1906. <https://doi.org/10.1007/s10529-012-0986-4>

Publisher's Note Springer Nature remains neutral with regard to jurisdictional claims in published maps and institutional affiliations.